Effect of magnetic interactions and multiple magnetic phases on the giant magnetoresistance of heterogeneous cobalt-silver thin films

J. F. Gregg
Clarendon Laboratory, University of Oxford, Parks Road, Oxford OX1 3PU, United Kingdom

S. M. Thompson
Department of Physics, University of York, Heslington, York YO1 5DD, United Kingdom

S. J. Dawson
Clarendon Laboratory, University of Oxford, Parks Road, Oxford OX1 3PU, United Kingdom

K. Ounadjela
Institut de Physique et Chímie des Matériaux de Strasbourg, Strasbourg, 4 rue Blaise Pascal, 67070 Strasbourg-Cedex, France

C. R. Staddon
Clarendon Laboratory, University of Oxford, Parks Road, Oxford OX1 3PU, United Kingdom

J. Hamman, C. Fermon, and G. Saux
Commissariat à l'Energie Atomique Saclay, 91191 Gif-sur-Yvette Cedex, France

K. O'Grady
SEES, University College North Wales, Bangor, Gwynedd, Wales
(Received 24 May 1993)

We have observed magnetic and electrical transport properties in giant magnetoresistive inhomogeneous cobalt-silver films. The material consists of two distinct magnetic phases: large clusters which dominate the magnetization and magnetoresistive processes at room temperature, between which cooperative behavior is observed; and small clusters which dominate the magnetization below 10 K, but make only a minor contribution to the magnetoresistance. Both the variation of the magnetoresistance with magnetization in the film and the difference in the magnetoresistance between the zero-field-cooled and field-cycled state are interpreted by invoking interactions between the active magnetic regions in the sample.

INTRODUCTION

Following the discovery of giant magnetoresistance in antiferromagnetically coupled multilayered films,[1] there has been extensive interest in their electrical transport and, in particular, their spin-dependent scattering properties. In such systems in which antiparallel alignment of the magnetic layers can be induced, spin-dependent scattering both at the magnetic/nonmagnetic interfaces and in the bulk of the magnetic layer results. This scattering is reduced as the layers are subsequently aligned in an applied magnetic field, producing a large or giant magnetoresistance effect which can be larger than 65%.[2] Such an effect is of significant interest in the design of magnetoresistive heads where previously, alloys such as NiFe have been used which have a magnetoresistance of only a few percent.[3] These studies have recently been extended to heterogeneous alloy systems[4–6] in which small amounts of a magnetic material are well dispersed in a nonmagnetic, metallic matrix and form single-domain magnetic regions. Spin-dependent scattering now originates from the randomly aligned single-domain regions in the sample as opposed to the magnetic layers in the multilayered films, and is a maximum at the point on the hysteresis curve where there is the greatest degree of misalignment. These metastable alloys can be prepared by a variety of techniques commonly used in commercial manufacture, such as sputtering, melt spinning,[7] and mechanical alloying.[8]

Previous workers have successfully interpreted their results on the assumption that there are no magnetic interactions.[4] In this investigation, material has been prepared and studied which exhibits similar properties to those already reported, but which differ in certain important respects. These measurements are described and discussed in the framework of a model incorporating local magnetic correlations and two distinct magnetic phases.

At equilibrium, cobalt is immiscible in silver,[9] however, by rapid quenching of these materials by processes such as sputtering onto ambient or low-temperature substrates, it is possible to inhibit phase separation. In the as-deposited state, the films generally tend toward single-phase metastable alloys,[10] however, ambient substrate temperatures and plasma bombardment during deposition may result in increased chemical short-range-order, producing cobalt-rich clusters. Subsequent annealing increases local fluctuations in the concentration of the magnetic species and eventually leads to phase segregation.

The magnetic properties of such systems are satisfactorily described by the model of Bean and Livingstone in which a superparamagnetic particle is defined as one which relaxes in a time less than the measurement time.[11] For a dc measurement, the time is generally taken to be 100 s, leading to the well-known criterion for the appearance of blocking,

$$KV_p = 25kT \ , \tag{1}$$

where K is the anisotropy energy density and V_p is the critical volume above which stable or blocked particle behavior is observed. The presence of blocked particles gives rise to hysteresis in the magnetization curve of the material.

The anisotropy is assumed to be uniaxial and may include contributions from magnetocrystalline and shape effects and in the case of our samples, the effects of intergranular coupling may give rise to a further effective anisotropy. For such uniaxial materials, if their axes are randomly oriented, the saturation remanence becomes half of the saturation magnetization when the temperature is such that all the moments are blocked.[12]

Thus, at most temperatures, a mixture of superparamagnetic and blocked particles are present in a given sample leading to complex behavior. Further, the intergranular coupling which may be both exchange and dipolar in nature, leads to complex magnetic behavior.[13]

In multilayer systems, the spin-dependent scattering arises both at the magnetic/nonmagnetic interface and in the bulk of the magnetic layer, depending on the material system. For cobalt/noble metal systems, the scattering has been found to be primarily due to interfacial scattering.[14] It is imperative that the electron mean-free path be longer than the thickness of the individual layers. This is particularly important for multilayers in which the current flows parallel to the film plane (CIP); the magnetoresistance obtained with the current flowing perpendicular to the plane (CPP) is much larger, but more difficult to measure due to the low resistivity of the multilayer stack. The case of granular systems is more comparable to the CPP situation,[15,16] in which the spin-flip diffusion length in the material must be longer than the interparticulate distance and the size of the particles themselves. The spin-independent scattering will be affected by the grain size, crystal defects, and impurities in the material. All these parameters will be modified during annealing of a well-dispersed, as-deposited sample owing to cobalt migration, increased grain size, sharper interfaces, improved crystallinity, and a reduced surface to volume ratio of the magnetic regions. This particle-size variation will also be seen in the magnetic response of the material and will ultimately result in large multidomain particles with no giant magnetoresistance.

SAMPLE DETAILS

The cobalt-silver films were grown on uncooled substrates by rf magnetron sputtering from a composite 50 mm diameter target. The target purities for cobalt and silver were 99.9 and 99.5 %, respectively. Once the system base pressure of 3.4×10^{-7} mbar had been reached, the target was presputtered at an argon pressure of 1.25×10^{-2} mbar and a power of 100 W. The 1000 Å films were deposited under identical sputtering conditions onto silicon wafers.

To obtain a range of alloy compositions under identical experimental conditions, a split sputtering target was used consisting of a semicircular cobalt foil mounted on a silver disk. By positioning the substrate perpendicular to the cobalt foil-silver target boundary, a clear composition gradient as determined by energy dispersive x-ray analysis (EDAX) was observed along the deposited film. The substrate was then divided into five pieces for further analysis.

ROOM-TEMPERATURE MEASUREMENTS

The magnetic properties were measured at room temperature using an alternating gradient force magnetometer with a maximum applied field of 2.2 T and a moment resolution of less than 2×10^{-8} emu. The transverse magnetoresistance was measured perpendicular to the concentration gradient in fields of up to 1.3 T using a standard four-point-probe method.

In the as-deposited state, the magnetic response of the samples (Fig. 1) showed typical fine particle behavior. The M-H loop is a sigmoidal curve with very small hys-

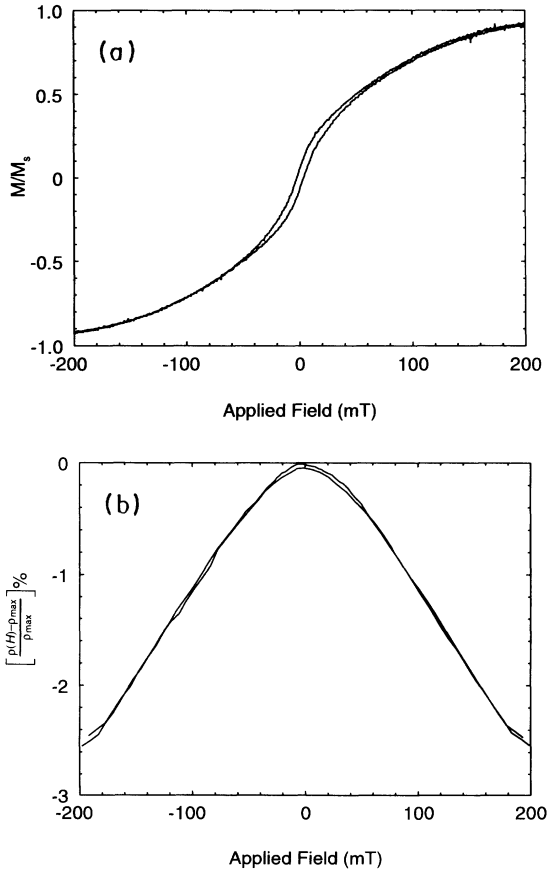

FIG. 1. Room-temperature characterization of as-deposited sample 2 (40 at % cobalt) (a) magnetization and (b) percentage magnetoresistance as a function of applied field. Expanded ±200 mT shown only.

teresis: remanence less than 10%. This is characteristic of a collection of unblocked single-domain particles, a small proportion of which have cooperative tendencies owing to the presence of net positive magnetic interactions.

In order to encourage phase segregation and the formation of larger cobalt-rich regions in the nonmagnetic matrix with higher blocking temperatures, one set of samples was annealed at 484 °C for 10 min. After this heat treatment, the samples displayed strongly hysteretic behavior with large coercive and remanent fields as shown in Fig. 2.

The maximum value of magnetoresistance obtained, defined as $(\rho_{max}-\rho_{min})/\rho_{max}$, was found to depend on the composition. Sample 2, which contains 40% cobalt, displayed the largest magnetoresistance of 10% at room temperature. The variation of maximum magnetoresistance as a function of position along the substrate and hence, decreasing cobalt content, is displayed in Fig. 3 for both the as-deposited and annealed samples. The increased particle size in the annealed films reduced the magnetoresistance, the maximum now being 1%. The sample in the series for which the maximum was obtained shifted to sample 3, a lower cobalt content sample.

The magnetoresistance of sample 2 at room temperature in the as-deposited state is displayed in Fig. 1(b). In this case, the magnetoresistance had a single peak with the maximum occurring at zero applied field where the magnetization of the sample passed through zero and the susceptibility is a maximum. The equivalent magnetoresistance curves for the annealed sample 3 are shown in Fig. 2(b). In this case, both the magnetization and resistance curves are hysteretic, with the maximum magnetoresistance occurring in the region of the coercive field where the magnetization again falls to zero.

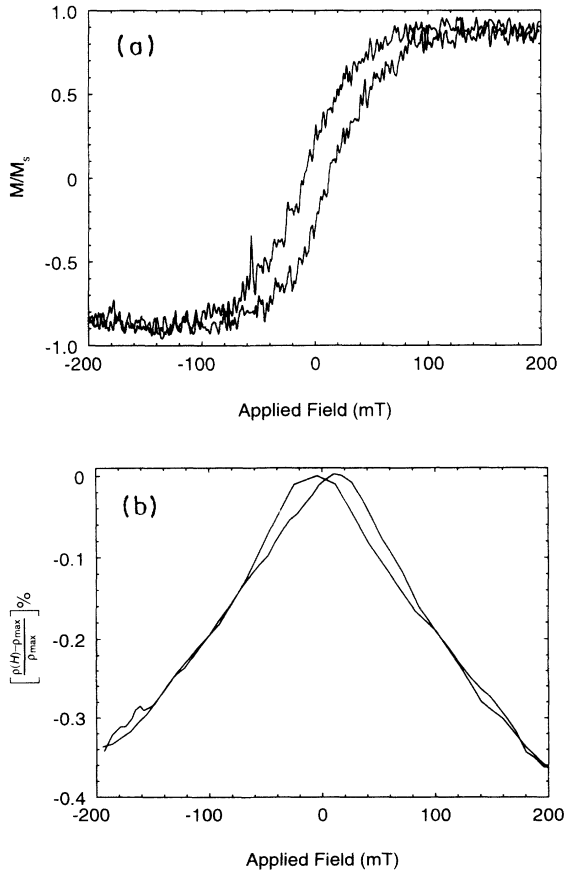

FIG. 2. Room-temperature characterization of annealed sample 3 (10 at % cobalt) (a) magnetization and (b) percentage magnetoresistance as a function of applied field. Expanded ±200 mT section shown only.

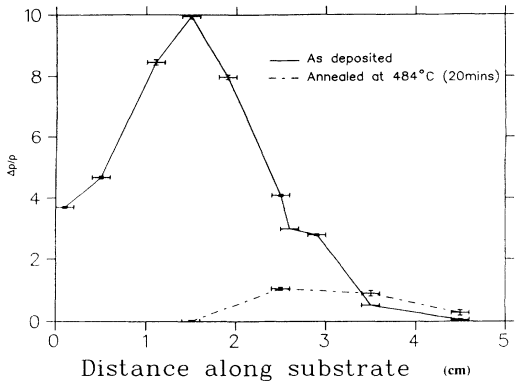

FIG. 3. Variation of room-temperature percentage magnetoresistance for both the as-deposited and annealed sample, with distance along the substrate corresponding to decreasing cobalt concentration.

LOW-TEMPERATURE MEASUREMENTS

Low-temperature magnetization measurements were made on the 40% cobalt sample using a superconducting quantum interference device (SQUID) magnetometer in fields up to 8 T. The hysteresis present in the as-deposited sample 2 remained constant until the measurement temperature was reduced below 100 K. It then increased rapidly on further cooling. This is best demonstrated in Fig. 4 by the decrease of the remanence on warming the sample from 4 K to room temperature.

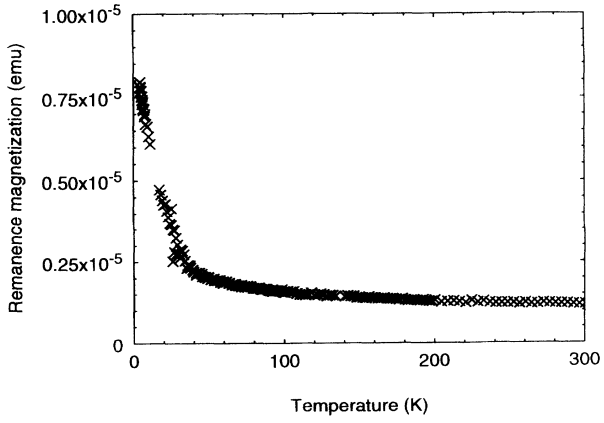

FIG. 4. Variation of remanence for as-deposited sample 2 (40 at % cobalt) with temperature. The sample was cooled to 2 K in a field of 8 T, which was then removed before measuring the magnetization as the temperature was increased.

Below 10 K there is a rapid increase in the low-field susceptibility and in the magnetization achieved by applying a large fixed field. This behavior is illustrated in Fig. 5(a) by the increase in magnetization with $H=4$ T as the sample was cooled and by the series of magnetization curves measured to 8 T at temperatures from 300 to 4 K in Fig. 5(b).

The magnetoresistance of the samples was measured, after cooling in zero field, at temperatures down to 4.2 K. The magnetoresistance increased as the measurement temperature was reduced, with the 40% cobalt sample 2 now producing 16% magnetoresistance at 4.2 K, as shown in Fig. 6. As the measurement temperature was reduced below 100 K, the magnetoresistance curve also became hysteretic with maximum values around the coercive field.

Immediately after cooling in zero applied field (ZFC) the samples exhibited a lower resistance than the maximum observed either at the coercive field, or at remanence after field cycling. The difference in the value of the percentage magnetoresistance in zero field immediately after cooling and the maximum magnetoresistance obtained during subsequent field cycling is defined as the quantity $\delta(\Delta\rho/\rho)$ and is marked in Fig. 6 for sample 2.

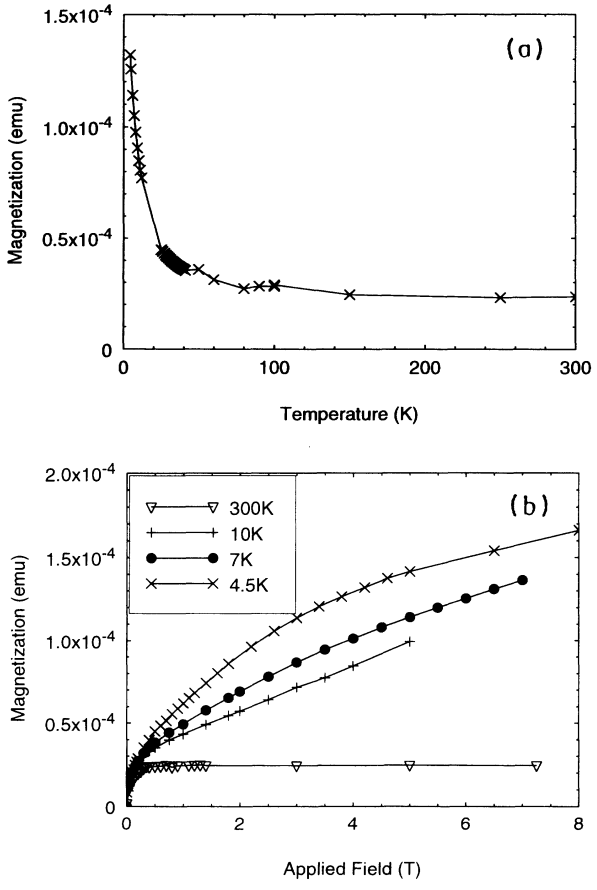

FIG. 5. (a) The increase in magnetization in an applied field of 4 T as the sample was cooled from 300 to 2 K for the as-deposited sample 2 (40 at % cobalt). (b) Magnetization as a function of applied field for the as-deposited sample 2 (40 at % cobalt) at measurement temperatures ranging from 4.5 to 300 K.

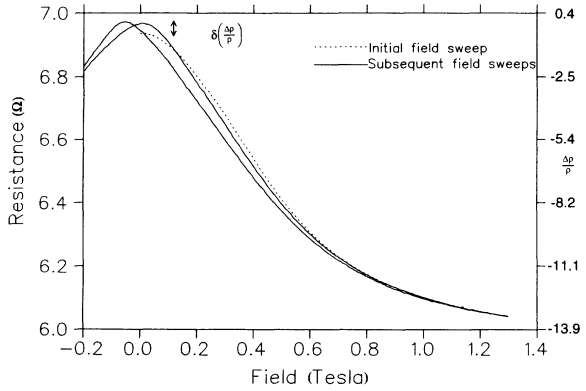

FIG. 6. The variation of resistance as a function of applied field at 4.2 K for the as-deposited sample 2 (40 at % cobalt) after cooling in zero applied field with the quantity $\delta(\Delta\rho/\rho)$ indicated.

$\delta(\Delta\rho/\rho)$ was positive below 100 K and its magnitude increased as the measurement temperature was reduced. The variation of $\delta(\Delta\rho/\rho)$ with temperature for the as-deposited sample 2 is plotted in Fig. 7.

DISCUSSION

The ideal as-deposited sample can be considered to consist of well distributed cobalt moments in a nonmagnetic silver matrix. These will be randomly distributed within each grain and may experience a range of interactions. Some moments may experience exchange coupling, causing them to form clusters of spins which will then behave effectively as a single "giant spin." The remaining interaction forces can now be considered to act either between individual moments or clusters of exchange-coupled moments. Following annealing, density fluctuations in the cobalt concentration will increase, eventually resulting in phase segregation to form cobalt-rich aggregates. Provided these regions are not so large that the formation of domain walls becomes energetically favorable, they can also be considered as single-domain particles between which interactions may occur.

Without forgetting the true inhomogeneous nature of the material, we shall treat single moments, clusters of

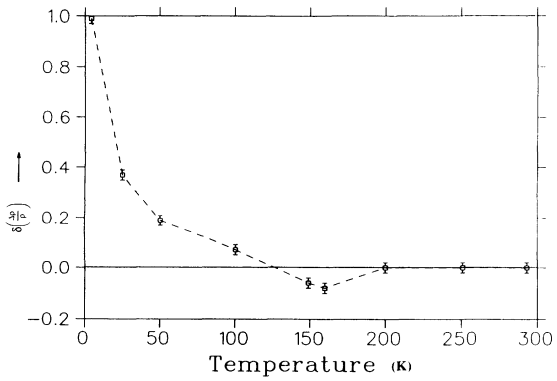

FIG. 7. The variation of $\delta(\Delta\rho/\rho)$ for the as-deposited sample 2 (40 at % cobalt) with measurement temperature.

moments, and aggregates as single-domain particles with a range of particle size and moment. Such an array of particles may behave as a superparamagnet with a characteristic blocking temperature distribution. If the interparticle distance is large enough, then no significant interactions will occur and the magnetization process will be governed by the anisotropy and volume of the individual particles.[17] For material with a high magnetic concentration, dipolar interactions will tend to align the moments of the particles to form flux-closure loops. Unlike particulate systems in a nonconducting matrix, the nonmagnetic matrix between the magnetic particles is metallic, and hence, can support Ruderman-Kittel-Kasuya-Yosida (RKKY) interactions which might be expected to couple adjacent magnetic particles of appropriate geometries. Such interactions could be either positive or negative depending on the interparticulate distance and configuration.

In giant magnetoresistive cobalt-based multilayers, the spin-dependent scattering is thought to occur primarily at the interfaces between the magnetic and nonmagnetic layers.[14] By analogy, in granular systems, the surface to volume ratio of the magnetic species is an important parameter, thereby giving rise to a dependence of magnetoresistance on particle size.[15,16] Moreover, there is an additional particle-size dependence, owing to the spin-flip diffusion length in the film defining a radius within which the spin-dependent scattering must occur. This dependence of magnetoresistance with particle size has been observed in cobalt-copper films by Berkowitz *et al.*[5]

The magnetic moment of a superparamagnetic material can be determined by fitting a weighted superposition of Langevin functions to the magnetization curve. Similarly, the blocking temperature distribution can be deduced from the variation of remanence with temperature. For a uniaxial system of particles with randomly oriented easy-axis directions, the remanence in the absence of thermal agitation is half the saturation magnetization.[12] As the sample is warmed, the remanence is reduced as those particles with lower anisotropy barriers become superparamagnetic, i.e.,

$$M_r(T)/M_s = 0.5 \frac{\int_{T_{BC}}^{\infty} f(T_B)dT_B}{\int_0^{\infty} f(T_B)dT_B} , \quad (2)$$

where $f(T_B)$ is the distribution of blocking temperatures. As discussed above, the blocking temperature for a particular class of particles of volume V is given by[11]

$$KV_p = 25kT_B . \quad (3)$$

Hence the distribution $f(T_B)$ can be obtained by simply differentiating Eq. (2).

The Langevin fit to the room-temperature magnetization curve is shown in Fig. 8. This fit and the narrow distribution of blocking temperatures evidenced by the sharp drop in remanence as the sample was warmed (Fig. 4), indicate that the clusters responsible for the room-temperature magnetization have a narrow moment distribution. The average moment of these clusters was calculated to be approximately $13\,000\mu_B$ which corresponds to a particle diameter of approximately 30 Å. Assuming these clusters have an anisotropy close to that of bulk hcp cobalt, we obtain a value of T_B of approximately 20 K for their blocking temperature, in satisfactory agreement with the behavior of $Mr(T)$ as in Fig. 4.

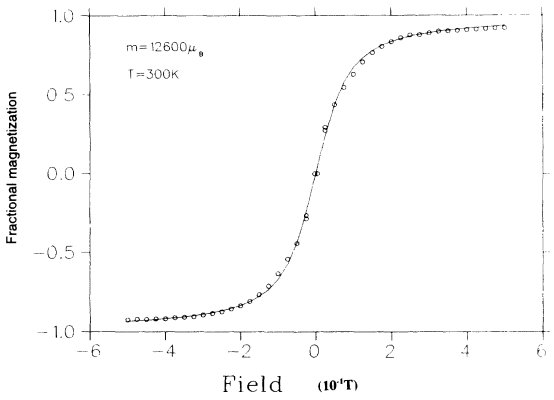

FIG. 8. Langevin fit to the room-temperature magnetization curve for the as-deposited sample 2 (40 at % cobalt). The continuous curve corresponds to a particle moment of $13\,000\mu_B$.

The low-temperature behavior of the large clusters can be separated from the magnetic response of the whole system. By fitting of Langevin functions to the data of Fig. 5(b), as shown plotted in Fig. 9, the sharp increase in magnetic moment between 10 and 4.5 K (of order five times that of the room-temperature value) is shown to be due to small superparamagnetic clusters of approximately four cobalt atoms. This low-temperature superparamagnetic behavior of the small clusters is also demonstrated by the superposition of the magnetization as a function of applied field divided by temperature curves as in Fig. 10, and the linear increase of susceptibility as a function of temperature as plotted in Fig. 11.

These two magnetic phases act almost independently with the large 30 Å clusters responsible for the room-temperature magnetization and magnetoresistance and

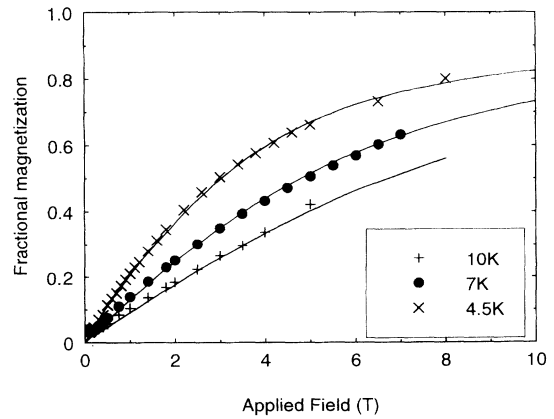

FIG. 9. Langevin fits to the low-temperature magnetization behavior of the as-deposited sample 2 (40 at % cobalt) having subtracted the predicted low-temperature response of the $13\,000\mu_B$ clusters. The continuous curve corresponds to a particle moment of $4\mu_B$.

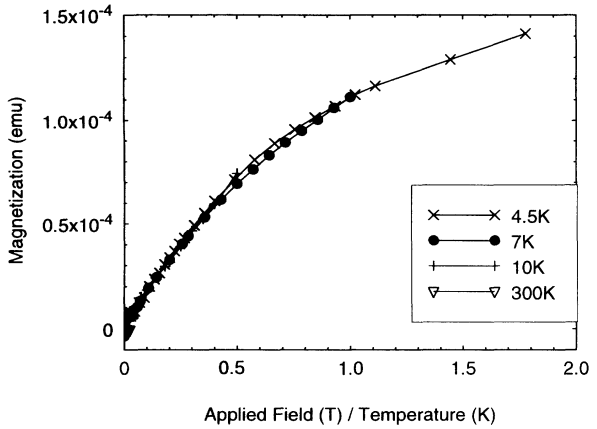

FIG. 10. The variation of magnetization with applied field/temperature for the as-deposited sample 2 (40 at % cobalt) at four measurement temperatures.

the small clusters dominating the low-temperature magnetization behavior and making a small contribution to the magnetoresistance.

We think it unlikely that the small room-temperature hysteresis could be due to a third phase of larger particles below their blocking temperature, as the variation of magnetization with temperature around room temperature is negligible [Fig. 5(a)]. This hysteresis may instead be due to ferromagnetic interactions between some of the large particles, a consequence of the relatively high cobalt concentration of our sample. These two phases may represent the as-deposited state with the cobalt atoms well dispersed throughout the matrix, but with some migration of cobalt to form the larger clusters. This may have occurred during growth owing to significant plasma bombardment because of the small target-substrate distance (4 cm). Transmission-electron microscopy is currently being employed to investigate the changes that occur during the annealing process.

Due to the particle-size dependence of the magnetoresistance, the small clusters are less efficient at spin-dependent scattering and hence, contribute less to the magnetoresistance than the larger clusters that are active

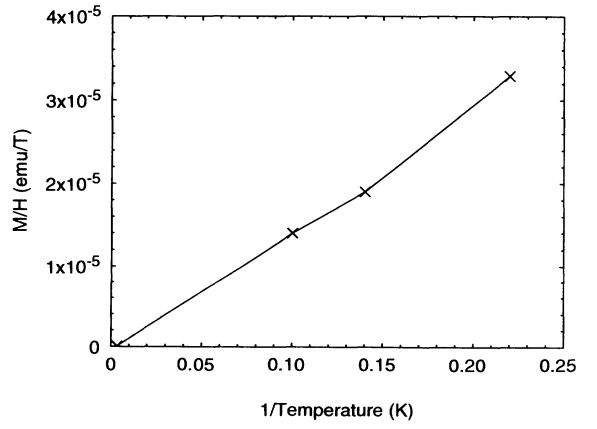

FIG. 11. Susceptibility as a function of temperature for the as-deposited sample 2 (40 at % cobalt).

at room temperature. The low-temperature magnetoresistance, such as that at 4 K (Fig. 6), displays an increased hysteresis which corresponds to the increasingly blocked large clusters and not the anhysteretic magnetization of the superparamagnetic small clusters. However, the resistance continues to decrease well above the applied field at which the large clusters are saturated, producing a long tail to the magnetoresistance (MR) curve such as has been observed, but unexplained, by other workers such as Xiao, Jiang, and Chien.[4] This long tail may correspond with the slow approach to saturation of the small clusters. The cobalt composition of our sample, at 40%, is relatively high and hence, the temperature for which the susceptibility of the small clusters becomes measurable is easily reachable at 10 K since they comprise about four to six interacting atoms. We suggest that previous observations have been made of lower cobalt-concentration samples for which the cluster sizes would be smaller and hence, would not appreciably polarize in the field and temperature ranges available.

Dieny *et al.*[18] have demonstrated, for an exchange-coupled multilayer in which they were able to vary the angle θ_{ij} between the magnetization directions in the layers by rotating the magnetization of one layer while pinning the other, that $(\Delta\rho/\rho)$ is proportional to $\cos\theta_{ij}$. By extension, a similar relation can be applied to the case of a granular system, $\langle \cos\theta_{ij} \rangle \alpha (\Delta\rho/\rho)$, where θ_{ij} is the angle between magnetic axes of any pair of particles i and j, and the average of the cosine is restricted to particles j lying within a sphere centered upon particle i and a radius of the electron mean-free path.

For parallel alignment of the magnetic particles (arising either from positive interactions or the application of an external magnetic field), $\langle \cos\theta_{ij} \rangle$ is positive and approaches unity with increasing alignment and when the magnetic correlation length is greater than the electron-scattering length.

For antiparallel alignment of adjacent particles, $\langle \cos\theta_{ij} \rangle$ is less than zero but approaches -1 only in the limit of small electron mean-free path of order the interparticle spacing. Antiparallel alignment and large electron mean-free path gives $\langle \cos\theta_{ij} \rangle$ approximately equal to zero as also does the case where both interactions and externally applied magnetic fields are absent and the magnetic moments are randomly orientated.

If the magnetization of our granular system proceeds by the rotation of single-domain particles, then the fractional magnetization M/Ms of the sample will be proportional to $\langle \cos\phi_i \rangle$, where ϕ_i is the angle between the moment of particle i and the magnetic field.

If there are no interactions between particles and their magnetic moments may be assumed to be completely randomly aligned, then a simple relation can be derived,[4] i.e.,

$$\langle \cos\phi_i \rangle^2 = \langle \cos\theta_{ij} \rangle \ .$$

This leads to the postulate,[4]

$$(M/Ms)^2 \alpha \langle \cos\phi_i \rangle^2 = \langle \cos\theta_{ij} \rangle \alpha (\Delta\rho/\rho) \ , \qquad (4)$$

for the case of no interactions. Relatively good agree-

ment with (4) was found at low temperatures by Xiao, Jiang, and Chien;[4] however, the room-temperature measurements made on our as-deposited samples deviated from the predicted quadratic. We interpret this as due to the presence of interparticle interactions and discuss the way in which these modify the simple relation (4) for a system above the blocking temperature of its constituent magnetic particles.

In a sample with magnetic interactions, the coupled regions have net moments which are determined by the balance of positive and negative interactions. When the sample is magnetized, different behavior is observed in the low- and high-field regimes. At low fields, the coupled regions of the sample reverse cooperatively, corresponding to coherent rotation of their constituent magnetic particles. This coherent rotation changes $\langle \cos\phi_i \rangle$ and hence M/Ms, but leaves $\langle \cos\theta_{ij} \rangle$ virtually unchanged since the relative angles between magnetic particle axes are maintained by the interactions even though the absolute orientations ϕ_i are being modified by the applied field. At larger fields, however, the individual magnetic particles become decoupled as the large external-field interaction with the particles begins to dominate over their mutual interaction and the system returns to the independent behavior described by Eq. (4).

When $(\Delta\rho/\rho)$ is plotted against $(M/M_s)^2$ for such a system, a distorted parabola such as that shown for sample 1 in Fig. 12 results which is characterized by a flat top; the position of whose "shoulders" are an indication of the local fields experienced by the particles due to their mutual interactions.

This quadratic will be further distorted at low temperatures when both magnetic phases are active with different values of saturation magnetization. Both phases may independently follow the quadratic relation (4), but it is difficult to separate their relative contributions, since this corresponds to the combination of two relations of form

$$(\Delta\rho/\rho)=\beta(M/Ms)^2 ,$$

which not only have different values of β and Ms, but whose fractional magnetizations are, moreover, very different at any particular value of applied field. When the system is magnetized, the larger particles align first at a modest value of the total magnetization fraction (since they account for only about 20% of the total saturation magnetization); however, they make a large contribution to $(\Delta\rho/\rho)$ since they are efficient spin-dependent scatterers. The result is a curve with a narrow central peak from the large particles, followed by a long tail at higher applied fields (Fig. 13). This corresponds to the rotation toward the field direction of the small clusters which make a less significant contribution to the magnetoresistance. This may also be a partial explanation for the small deviation from the equivalent quadratic formula by Xiao, Jiang, and Chien[4] at 5 K.

It is worth noting that, unlike the high-temperature parabola (Fig. 12), the low-temperature version (Fig. 13) no longer has a flat top, indicating the effective suppression at low temperatures of the interparticle interactions as discussed later.

As the spin-dependent scattering depends on the relative orientations of the moments of the single-domain particles, the greater the degree of antiparallel alignment on the same scale as the scattering length, and the greater the spin-dependent scattering as measured by $(\Delta\rho/\rho)$. The point of the magnetization process that results in the greatest degree of antiparallel alignment will also, therefore, be the point of maximum $(\Delta\rho/\rho)$. Hence, it is worth considering the various different magnetic configurations in which the sample might find itself in a zero magnetization state and what differences can be expected in the corresponding values of $(\Delta\rho/\rho)$. In the anhysteretic state above the blocking temperature of a set of noninteracting superparamagnetic samples, true random alignment of the magnetic moments can be expected at zero applied field. However, in our samples, both positive and negative interactions are present with those of positive sign clearly dominating, as seen from the discussion below. We now consider the consequences of such interparticle interactions on the microscopic magnetic configuration of the zero magnetization state and also how such a system behaves when cooled and subjected to field cycling.

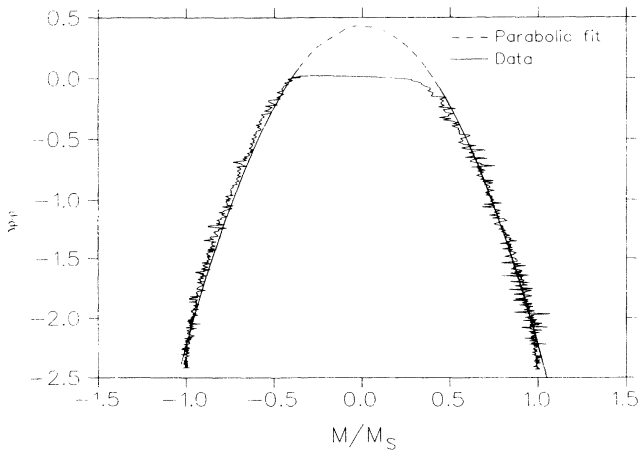

FIG. 12. The variation of percentage magnetoresistance with fractional magnetization at 300 K for the as-deposited sample 1 (35 at % cobalt).

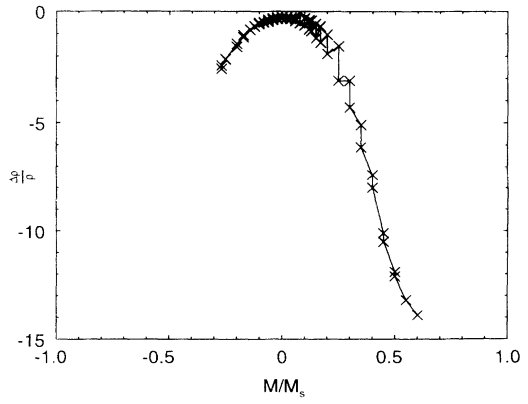

FIG. 13. The variation of percentage magnetoresistance with fractional magnetization at 4.5 K for the as-deposited sample 1 (40 at % cobalt).

When cooled from room temperature in zero field, the sample displayed a difference between the resistance measured in zero field immediately following cooling and that measured at zero field or at zero magnetization following field cycling to 1.4 T and back, i.e., the $\delta(\Delta\rho/\rho)$ effect. This discrepancy first became evident at 175 K where it was negative (i.e., the maximum field-cycled resistance was less than the initial resistance) as observed in previous work on both multilayers and alloys.[19,4] On further lowering the temperature at which the field was swept and the magnetoresistance measurements made, the effect was found to change sign to become positive at 100 K and its magnitude increased sharply on cooling below 50 K.

The key to this behavior lies in the striking similarity between the temperature dependence of $\delta(\Delta\rho/\rho)$ and that of the remanence Mr, both of which are plotted for comparison in Fig. 14. The remanence $Mr(T)$ arises from progressive blocking of the large (approximately 30 Å) single-domain particles as the sample is cooled. These particles are subject to interactions which may be dipolar, or RKKY in origin and are likely to be of both signs. At high temperatures, the interactions induce correlations between the moment directions of adjacent superparamagnetic particles with the consequence that the magnetic configuration is not completely random and the value of $\langle \cos\theta_{ij} \rangle$ differs from zero (either positively or negatively) as discussed previously.

On cooling in zero field, these correlations are retained. However, at the measurement temperature some of the magnetic particles are now blocked, and for them the influence of the interparticle interactions is effectively suppressed once the sample has been subjected to field cycling. Consequently, when the field is swept to magnetic saturation and then returned to the dc demagnetized state, the net moment is zero as for the zero-field-cooled demagnetized state, but the microscopic particle-moment distribution is different: this is because the magnetic configuration of those particles which are below their blocking temperatures is now determined not by the interactions, but by particle volume, crystal and shape anisotropies, and surface effects. These may be expected to be completely random, thereby giving rise to a more random magnetic-moment configuration than before the field sweep.

The sign of $\delta(\Delta\rho/\rho)$ depends on whether the interactions suppressed by cooling are positive or negative. It is seen from Fig. 7 that in our sample, the small number of particles at the upper end of the blocking temperature spectrum ($T_b \sim 150$ K) seem predominantly subject to negative interactions, hence the small negative excursion of $\delta(\Delta\rho/\rho)$ around 150 K. Those with lower blocking temperatures ($T_b < 100$ K) which account for the bulk of the large particle magnetization are positively coupled, thereby producing a positive $\delta(\Delta\rho/\rho)$ at lower temperatures. As the sample is cooled to 4 K, a progressively larger fraction of these particles block, giving rise to the observed dramatic increase in the $\delta(\Delta\rho/\rho)$ effect, which mirrors the increase in $Mr(T)$ as described above and shown in Fig. 14.

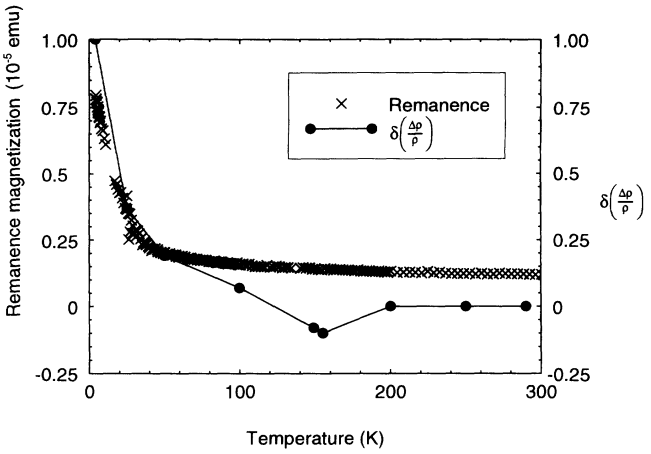

FIG. 14. Comparison of the variation of remanence and $\delta(\Delta\rho/\rho)$ with temperature for the as-deposited sample 1 (40 at % cobalt).

CONCLUSION

Giant magnetoresistance of 16% at 4 K has been observed in inhomogeneous cobalt-silver thin films. The films were found to consist of two magnetic phases: small clusters of approximately four cobalt atoms which do not begin to align in available laboratory fields until the temperature is reduced below 10 K and which contribute less to the giant magnetoresistance than the second phase of large 30 Å cobalt clusters which dominate the room-temperature magnetic and magnetoresistance behavior. Cooperative behavior of these larger clusters was found to be responsible for differences between the resistance in the zero-field-cooled state and at zero field or zero magnetization during subsequent field cycling. These positive interactions were also found to result in deviations from the quadratic relation predicted between M/Ms^2 and $(\Delta\rho/\rho)$ for noninteracting particles. At low temperatures, this relation was further distorted by the active presence of the two magnetic phases. The relatively high cobalt concentration in our sample may have made these effects more readily accessible than in the lower cobalt concentration samples of other workers.

ACKNOWLEDGMENTS

Financial support from the SERC, Royal Society, and British Council is gratefully acknowledged. A. Herr and R. Poinsot are thanked for assistance with the SQUID magnetometry.

[1]M. N. Baibich, J. M. Broto, A. Fert, F. Nguyen Van Dau, F. Petroff, P. Etienne, G. Creuzet, A. Friederich, and J. Chazelas, Phys. Lett. B **61**, 2472 (1988).

[2]S. S. P. Parkin, Appl. Phys. Lett. **60**, 512 (1992).

[3]B. Rodmacq, G. Palumbo, and Ph. Gerard, J. Magn. Magn. Mater. **118**, L11 (1993); J. Mouchot, P. Gerard, and B. Rodmacq (unpublished).

[4]J. Q. Ziao, J. S. Jiang, and C. L. Chien, Phys. Rev. Lett. **68**, 3749 (1992).

[5]A. E. Berkowitz, J. R. Mitchell, M. J. Carey, A. P. Young, S. Zhang, F. E. Spada, F. T. Parker, A. Hutten, and G. Thomas, Phys. Rev. Lett. **68**, 3745 (1992).

[6]J. A. Barnard, A. Waknis, M. Tan, E. Haftek, M. R. Parker, and M. L. Watson, J. Magn. Magn. Mater. **114**, L230 (1992).

[7]J. Wecker, R. von Helmolt, L. Schultz, and K. Samwer, Appl. Phys. Lett. **62**, 1985 (1993); R. Ferrer, B. Barbara, B. Dieny, A. Chamberod, C. Cowache, J. B. Genin, and S. Teixeira (unpublished).

[8]S. M. Thompson, J. F. Gregg, C. R. Staddon, D. Daniel, S. J. Dawson, K. Ounadjela, J. Hamman, C. Fermon, G. Saux, K. O'Grady, J. M. D. Coey, and A. Fagan, Philos. Mag. B (to be published).

[9]M. Hansen, *Constitution of Binary Alloys* (McGraw-Hill, New York, 1958), p. 16.

[10]M. L. Watson, J. A. Barnard, S. Hossain, and M. R. Parker, J. Appl. Phys. **73**, 5506 (1993).

[11]C. P. Bean and J. D. Livingstone, J. Appl. Phys. **30**, 120S (1959).

[12]E. C. Stoner and E. P. Wohlfarth, Philos. Trans. R. Soc. London, Ser. A **240**, 599 (1948).

[13]K. O'Grady (unpublished).

[14]B. Dieny, J. Phys. Condens. Matter **4**, 1 (1992); W. P. Pratt, Jr., S. F. Lee, Q. Yang, P. Holody, R. Lolee, P. A. Schroeder, and J. Bass, J. Appl. Phys. **73**, 5326 (1993).

[15]S. Zhang, Appl. Phys. Lett. **61**. 855 (1992).

[16]B. Dieny, S. R. Teixeira, B. Rodmacq, C. Cowache, S. Auffret, O. Redon, and J. Pierre (unpublished).

[17]I. S. Jacobs and C. P. Bean, in *Magnetism,* edited by G. T. Rado and H. Suhl (Academic, New York, 1963), Vol. III, pp. 271–350.

[18]B. Dieny, V. S. Speriosu, S. S. P. Parkin, B. A. Gurney, D. R. Wilhoit, and D. Mauri, Phys. Rev. B **43**, 1297 (1991).

[19]W. P. Pratt, Jr., S. F. Lee, J. M. Slaughter, R. Loloee, P. A. Schroeder, and J. Bass, Phys. Rev. Lett. **66**, 3060 (1991).